MDPI

Coastal Vulnerability Impact Assessment under Climate Change in the Arctic Coasts of Tromsø, Norway

Polyxeni Toumasi [1], George P. Petropoulos [1,*], Spyridon E. Detsikas [1], Kleomenis Kalogeropoulos [2] and Nektarios Georgios Tselos [1]

[1] Department of Geography, Harokopio University of Athens, El. Venizelou St., 70, 17671 Athens, Greece; ptoumasi@hua.gr (P.T.); sdetsikas@hua.gr (S.E.D.); gs21966@hua.gr (N.G.T.)

[2] Department of Surveying and Geoinformatics Engineering, University of West Attica, Ag. Spyridonos Str., 12243 Athens, Greece; kkalogeropoulos@uniwa.gr

* Correspondence: gpetropoulos@hua.gr; Tel.: +30-2109549163

Abstract: Arctic coastlines are the most vulnerable regions of the Earth, and local communities in those areas are being affected by rising sea levels and temperature. Therefore, Earth Observation combined with up-to-date geoinformation tools offers a dependable, cost-effective, and time-efficient approach to understanding the socioeconomic impact of climate changes in Arctic coastal areas. A promising approach is the Coastal Vulnerability Index (CVI), which takes into account different factors such as geomorphology, sea factors, and shoreline retreat or advance, to estimate the grade of vulnerability of a coastal area. Notwithstanding its potential, its application in the Arctic is still challenging. This study targets to estimate CVI to value the vulnerability of the coastal areas of Norway located in the Arctic. For the application of CVI and specifically for geomorphological and sea factors, data were acquired from international and national institutes. After the collection of all the necessary parameters for CVI was completed, all datasets were imported into a GIS software program (ArcGIS Pro) where the vulnerability classes of CVI were estimated. The results show that most of the coast of Northern Norway is characterized by a low to high degree of vulnerability, while in the island of Tromsø the vulnerability is mainly high and very high.

Keywords: Coastal Vulnerability Index; remote sensing; Arctic; Tromsø; Norway; GIS; EO-PERSIST

1. Introduction

The Arctic region is acutely endangered by climate change, warming at a rate three times faster than the global average. The consequences of climate change, such as escalating sea levels, thawing permafrost, diminishing sea ice, and melting glaciers, significantly imperil Arctic coasts, rendering them extremely vulnerable [1]. Changes in permafrost lead to significant ecological as well as economic impacts on a global scale [2,3]. Rising sea levels and temperature have detrimental effects on the local communities, negatively affecting coastal infrastructures [3]. Therefore, it is of key importance to assess the degree of Arctic coastal vulnerability to both physical and socioeconomic factors, as this is key to monitoring the impacts of climate change on local communities [4].

A particularly promising methodology in evaluating the vulnerability of Arctic coasts is a multivariate geospatial index, the so-called Coastal Vulnerability Index (CVI). CVI expresses the degree of vulnerability of a coastline by taking into consideration different physical factors such as geomorphology, oceanographic factors (sea level rise, wave height, and tidal range), and shoreline retreat or advance to estimate the degree of vulnerability of a coastal area. Coupling CVI with advanced geoinformation tools [5], including Earth Observation imagery, unmanned aerial vehicles that enable data collection from a safe distance [6], innovative sensors like LiDAR-based systems

[7,8], and cutting-edge techniques such as deep learning models, provides more valuable insights into the state of the Arctic zone [9], thus having the potential to improve our understanding about Arctic coasts dynamics. This index is important for identifying coastal segments and infrastructures as well as other activities that are essentially susceptible to the risk posed by different physical factors [10]. Amongst the most significant advantages of the CVI is the fact that the index is highly customizable, as it is feasible to fuse it with different physical and socioeconomic factors, and it is highly adaptable to different settings [11]. CVI has been extensively applied to various environmental settings (e.g., refs. [12–14]), but its application in the Arctic is yet underexplored with only a limited number of studies existing [15].

In this context, this study aims to estimate the CVI to evaluate the vulnerability of the coastal areas of Norway located in the Arctic and specifically for the island of Tromsø. For the application of CVI and particularly for the geomorphological and sea factors, data were acquired from international and national institutes. For assessing coastal erosion/deposition rates, Landsat satellite images for the years 1993 and 2023 were used.

2. Study Area

Situated north of the Arctic Circle, and specifically at 69° northern latitude [16], the island-city of Tromsø is the most populated city in Northern Norway [17]. According to Statistics Norway (2022), Tromsø has a blooming population of 77,544 [18]. This affluent Arctic capital is linked to the mainland by the Tromsø Bridge and Tromsøysund Tunnel. Tromsø is not only the most populated city in Northern Norway, it is also the largest city, and it is situated approximately 400 km north of the Arctic Circle. Tromsø is characterized by two months of midnight sun and two months of polar night. Nonetheless, according to Jacobsen et al., because of the Gulf Stream, the climate is relatively mild [19]. In order to detect the land uses of Tromsø, the use of the Corine Land Cover (https://land.copernicus.eu, accessed on 10 October 2024) was helpful. According to Corine, the largest part of Tromsø is covered by urban fabric, while immediately after are mixed forests.

A diverse combination of physical factors are exhibited in mainland Norway, resulting in a variety of climate conditions. According to Ketzler et al. [20], Norway covers five climate zones (Köppen classification). Being located on the west side of the Scandinavian Peninsula, the North Atlantic Current moderates the climate to a more temperate level than what it is expected from the given geographical zone. Specifically, a notable temperature increase has been detected over the past two decades. In Northern Norway, the high mountain plateaus have a subarctic appearance, including permafrost phenomena. It is notable that some parts of Norway lack both vegetation and soil, but they are covered by block accumulations with vertical extensions occasionally reaching several meters, with an absence of finer material between the blocks. Regarding the effects of sea level rise, only minor effects are anticipated for the Norwegian coast during this century. More specifically, there will be increases up to 0.6 m in some areas, largely offset by a postglacial rebound. The number of days with snow cover will potentially decrease significantly across Norway by up to 180 days per year. Climate models suggest that permafrost in areas like Finnmarksvidda may completely defrost by 2050 and only some small permafrost areas that are in mountainous areas over 1800 m a.s.l will be able to remain [20]. Tromsø (Figure 1) is an elongated NNE–SSW-striking basin, with a length of 140 km and a width of 60 km [21].
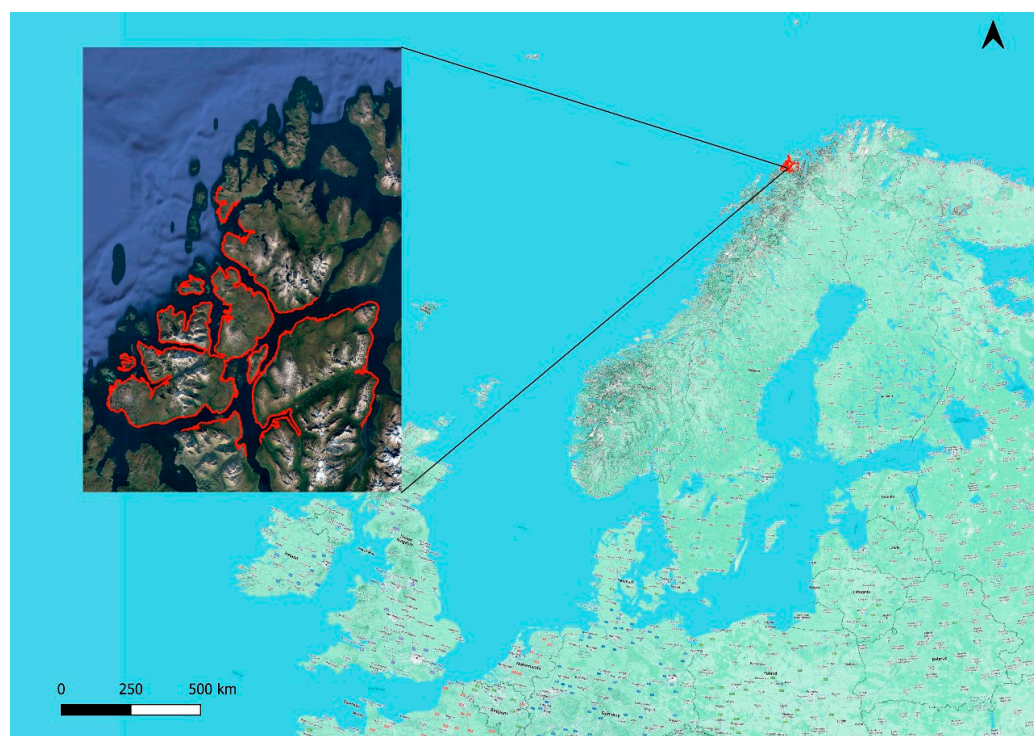
Figure 1. The geographical location of Tromsø Municipality. Red line depicts the municipality borders (Tromsø, Norway).

2.1. CVI Variables

For the estimation of CVI, six variables linked to natural characteristics and physical processes (geomorphology, slope, shoreline change, oceanographic conditions) were considered in reflecting the coastal vulnerability in the study area. A summary of the dataset used is presented in Table 1. Below, an analytical description of each variable used for the estimation of CVI is presented.

Table 1. Data sources used in CVI calculations in this study.

Variable	Data Source	Reference Period
Geomorphology	Global Lithological Map www.geo.uni-hamburg.de (accessed on 10 October 2024)	-
Coastal slope	Copernicus DEM https://search. earthdata.nasa.gov/search (accessed on 10 October 2024)	-
Shoreline erosion/accretion (m/yr)	Landsat 5 TM and 9 OLI2	1993 & 2023
Relative sea level change (mm/yr)	Norwegian Hydrographic Services Mapping Authority api.sehavniva.no	1993–2024
Mean tide range (m)	Norwegian Hydrographic Services Mapping Authority api.sehavniva.no	1993–2024
Mean wave height (m)	Based on literature	1993–2024

2.1.1. Shoreline Change

To monitor the coastline deposition/erosion rates over the selected region and the selected period, remotely sensed imagery from Landsat satellite program archive was used. Landsat is the longest existing optical earth observation program with an almost continuous archive to date and a moderate pixel size (30 m spatial resolution) from 1972

coordinated by NASA and the U.S. Geological Survey. Landsat data were found to be ideal for this study, as the extensive and consistent archive has been widely used in coastline dynamics monitoring (e.g., refs. [22,23]). More specifically, imagery from Landsat 5 on 23 August 1993 and Landsat 9 on 30 June 2023 was used to fulfill the objectives of this study. Multi-date image acquisition was chosen, as it allows for the exploitation of change detection techniques regarding coastal changes. The images were obtained at Surface Reflectance Level 1 and cropped to the extent of Tromsø Municipality. Only the VNIR and SWIR spectral bands were used from the Landsat satellites, as the corresponding thermal bands from each sensor were excluded from the analysis. The coastline of 2023 was used as the basis for the calculation of all the other factors of the index, respectively. Similar surveys have calculated this factor in the same way [24,25].

2.1.2. Geomorphology

Geomorphology is a critical component of CVI, as it is linked to the risk of erodibility and, consequently, the overall degree of the coast's physical vulnerability. Usually, geomorphological mapping is performed via direct field observations and coastal geomorphological mapping of the examined area. However, these activities are particularly time-consuming and labor-intensive, especially when performed over large geographic areas. Therefore, utilizing high-resolution satellite imagery and other geological geospatial reference maps poses as a cost-effective alternative for acquiring geomorphological information. In this study, geomorphological mapping was performed utilizing high-resolution aerial imagery accessed from Norgebilder (https://www.norgeibilder.no/?id=3502, accessed on 5 September 2024). Furthermore, as an auxiliary dataset, the Global Lithological Map (GLiM) was used to assess the erodibility risk of the lithological coastal zone in the examined area [26]. It was found that the coastal zone was mainly characterized by metamorphic formations as well as acid and basic plutonic rocks, formations known as erosion-resistant geological formations, indicating a low risk level of vulnerability.

2.1.3. Coastal Slope

The coastal slope indicates both the relative risk of inundation as well as the potential rate of shoreline retreat [27]. For the coastal slope factor, the Copernicus Digital Elevation Model (DEM) was used. Copernicus DEM was released in 2020 and is derived from WorldDEM data. The WorldDEM data product is based on radar satellite data which were acquired during the TanDEM-X mission. The duration of the TanDEM-X data acquisition was between December 2010 and January 2015. The Copernicus GLO-30 dataset has a grid spacing of 1 arc-second (30 m) and is available at a standardized extent of $1° \times 1°$.

2.1.4. Oceanographic Parameters

Regarding the oceanographic conditions of the area, three parameters were taken into consideration during the CVI estimation. Those consist of (i) the relative sea level change of the examined area expressed in units of millimeters per year (mm/yr), (ii) the mean tide range expressed in meters, and (iii) the mean wave height conditions expressed also in meters. Data about the relative sea level rise and mean tidal range between 1993 and 2024 were obtained by a tide gauge station installed at the harbor of Tromsø available through the Norwegian Hydrographic Services Mapping Authority database (api.sehavniva.no, accessed on 10 October 2024). Regarding mean wave height, a value of 1.0 m was selected based on the physiographical characteristics of the wider area and in accordance with other similar studies which took place in the wider geographical area [28].

3. Methodology

To satisfy the study objectives, there was the pre-processing stage and the processing stage. All the steps followed for the implementation of the study can be seen in the flowchart below (Figure 2).
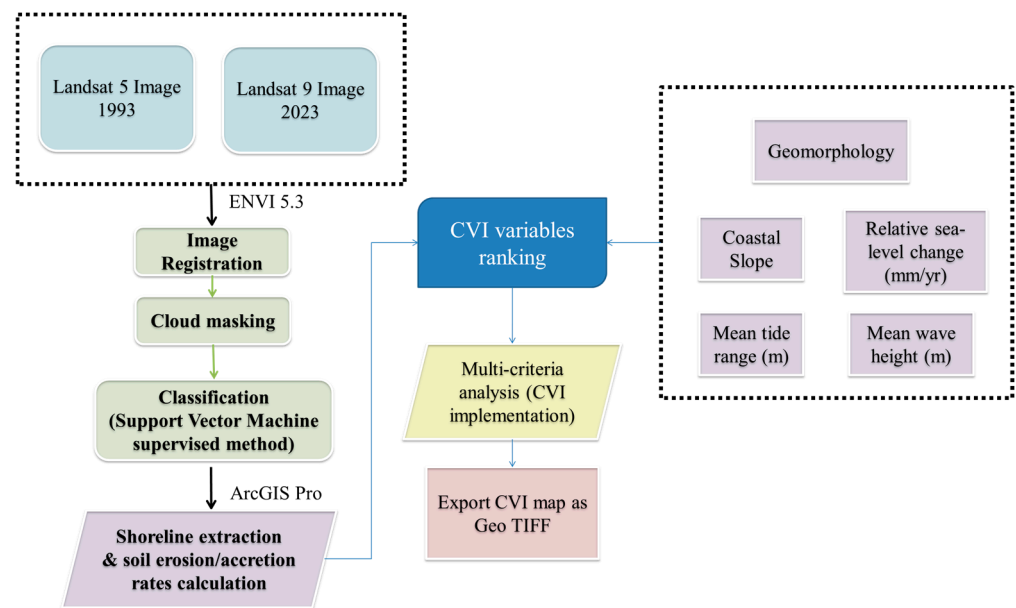
Figure 2. Flowchart of the methodology used in this study.

3.1. Shoreline Extraction

ENVI Classic 5.3 software was used for image processing. In order to extract the coastline position for those two years, the modified Normalized Difference Water Index was estimated to delineate land from water while standard GIS operations were used to extract the erosion/deposition rates. Upon the achievement of gathering all the necessary parameters for CVI, all datasets were imported into GIS software, and specifically ArcGIS Pro, where the vulnerability classes of CVI were estimated. The first step in ENVI Classic was the image registration to geometrically align the two overlapping images. Then cloud masking was applied to the images to remove the existing clouds. For each of the satellite images, ROIs were obtained. The ROIs were used to later classify data. For the objectives of this research, 2 classes were created (sea and land). The classification method used was Support Vector Machines (SVMs) [29]. The use of SVMs was the more appropriate, because even with small sample sizes, proper estimates of the prediction error can be produced. Moreover, SVM classification allows for the avoidance of the degradation of computational performance that may occur in high dimensions [30].

3.2. CVI Estimation

After the pre-processing of the images in ENVI software was finished, the images, which were all at 30 m spatial resolution, were then processed in ArcGIS Pro software (Version 3.1). In this particular program, the shoreline extraction and soil erosion/accretion rates calculation was carried out. The factors used to calculate the CVI were six. Specifically, those factors were geomorphology, coastal slope, mean tide range (m), shoreline erosion/accretion (m/yr), relative sea level change (mm/yr), and mean wave height (m). The above variables took integer values ranging from one (1) to five (5). Each of the parameters was categorized based on the potential contribution they have to the natural changes of the coast, as the sea level rises [31]. The higher the value, the more vulnerable the areas are to that parameter. A multi-criteria analysis was applied for CVI implementation. In more detail, initially each factor was calculated separately, with the format of the files being in vectors (polylines). To classify each factor in each of the 5 categories, according to their vulnerability, Table 2 was used.

Table 2. CVI variables ranked into five categories [15].

Vulnerability Parameter	Very Low 1	Low 2	Moderate 3	High 4	Very High 5
Geomorphology	Rocky, cliffed coast, fjords, fiards	Medium cliffs, indented coasts	Low cliffs, glacial drift, alluvial plains	Cobble beaches, estuary	Barrier beaches, sand beaches, deltas, sand spits
Coastal slope (°)	>10.0	6.0–10.0	3.1–6.0	1.0–3.0	<1.0
Relative sea level change (mm/yr)	<1.8	1.8–2.5	2.5–2.95	2.95–3.16	>3.16
Shoreline erosion/accretion (m/yr)	>2.0	1.0–2.0	(−1.0)–(+1.0)	(−1.1)–(−2.0)	<−2.0
Mean tide range (m)	>6.0	4.1–6.0	2.0–4.0	1.0–1.9	<1.0
Mean wave height (m)	<0.55	0.55–0.85	0.85–1.05	1.05–1.25	>1.25

For the creation of sea level rise map and for the map of mean tide range, data from 1993 to 2024 were used, which were hourly for each day of the year, for all years of the under-study time period. After finding the average of each factor for each year, the value was then calculated for the range covered by the paper, i.e., for the period of 1993–2023. The value was then entered into the GIS software, and the appropriate level of hazard was obtained according to Table 2. To create the coastline advance/subsidence map, two coastlines were used, one for the year 2023, which is also the basis on which the rest of the maps of the factors were made, and a coastline for 1993. The reason that only the years 1993 and 2023 were used is that the CVI formula specifies that the first and last year of the study period must be used to calculate the shoreline retreat/advance factor. By choosing two dates that are 30 years apart, the analysis emphasizes long-term, significant changes rather than shorter-term fluctuations, which might not reflect lasting trends. This approach provides a clearer picture of cumulative shoreline evolution over time which is also what is needed to calculate CVI. Initially, the 2023 coastline was divided into equal parts. Then the distance of each part of the coastline from the oldest coastline was calculated and then the rate of change in meters per year. The next step was to identify the cases of advance and retreat (1 for the values where there was advance and −1 for the values where there was retreat). After a buffer was created, segments that had advance or retreat were selected accordingly. Finally, by combining the data retrieved from the rate of change per year and the field containing the values 1 (advancement) and −1 (recession), as well as using Table 2, a categorization was made for each value of the specific factor, regarding their vulnerability. A multi-criteria analysis was applied. The weighting factors of each individual parameter were decided on the basis of relevant literature and studies in arctic regions. In line with corresponding studies, all variables were given equal weight [24,32–34]. For the geomorphology factor, the lithology of each area was categorized based on the general category they belong to, and then, using Table 2, the rocks were ranked based on their vulnerability. As for the coastal slope factor, a TIN file was created, and then a Triangle TIN file (in degrees). The next step was the segmentation of the coastline based on the coastal gradients. Based on Table 2, each value was categorized according to the level of vulnerability it had.

Each factor was exported as a vector file. Then the vector files were converted to raster. This conversion was necessary in order to be able to calculate the CVI (Equation (1)) using the raster calculator tool in ArcGIS Pro through the mathematical expression shown below. Lastly, the final CVI map was exported as Geo TIFF. The above methodology is also shown in the flowchart in Figure 2.

$$CVI = \sqrt{\frac{a \times b \times c \times d \times e \times f}{6}} \tag{1}$$

where a = geomorphology, b = shoreline change rates, c = coastal slope, d = relative sea level rate, e = mean significant wave height, and f = mean tidal range.

4. Results

Regarding the vulnerability of each factor used to calculate CVI, with reference to the mean wave height factor, the vulnerability throughout the coastline was moderate, as can be seen from the corresponding Figure below (Figure 3), as well as in Figure 4f. In regard to the mean tidal range, the vulnerability seems to be very high (Figures 3 and 4e, as for the factor of relative sea level rise (Figures 3 and 4b), contrary to the factor of geomorphology (Figures 3 and 4a), regarding which, due to the type of rocks that cover the area, the vulnerability is very low. In relation to the coastal slope factor (Figures 3 and 4d), vulnerability is generally high (49.1% out of the total coastline), while the next largest percentage of the coastline corresponds to very low vulnerability (approximately 27% out of the total coastline). Finally, in the shoreline erosion/accretion factor, the vulnerability is mainly moderate (approximately 55% out of the total coastline) (Figures 3 and 4c). The above results can be seen diagrammatically in the Figure below (Figure 3). Furthermore, the vulnerability of each parameter can be shown in Figure 3, where all the factors of CVI in individual maps are presented. In addition, those percentages do not only concern the Tromsø area but cover a larger area, as can be seen on the map below (Figure 4).

As can be seen from Figure 4c, as far as the shoreline erosion/accretion factor is concerned, very high vulnerability is observed in the central part of the map, as well as on the western part of the coastline. Also, in the western part of the island of Tromsø, a very high vulnerability to this factor is found, in contrast to the eastern part, where mainly moderate vulnerability is observed. Along the northern part of the coastline, it is clear that the coastline is mostly very high and moderate. As for the central part of the map, as well as the southern part, there are points of the coastline where vulnerability is very low, as well as on the eastern part of the coastline. In the part of the coastline to the east of the island of Tromsø, the vulnerability is mainly very high, in contrast to the part of the coastline located to the west of the island of Tromsø, where the vulnerability regarding the shoreline erosion/accretion factor is very low and occasionally moderate.
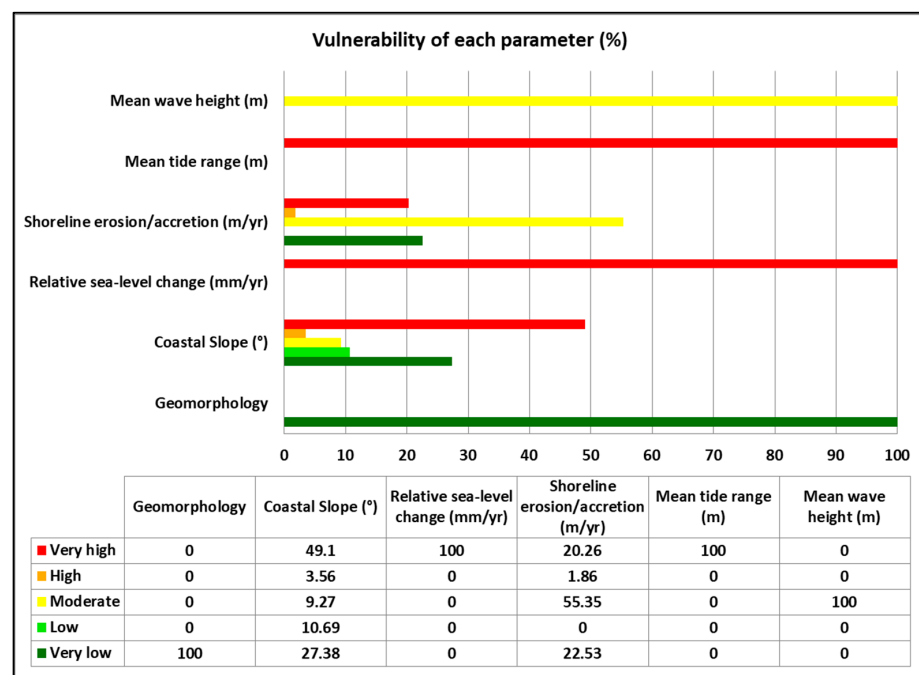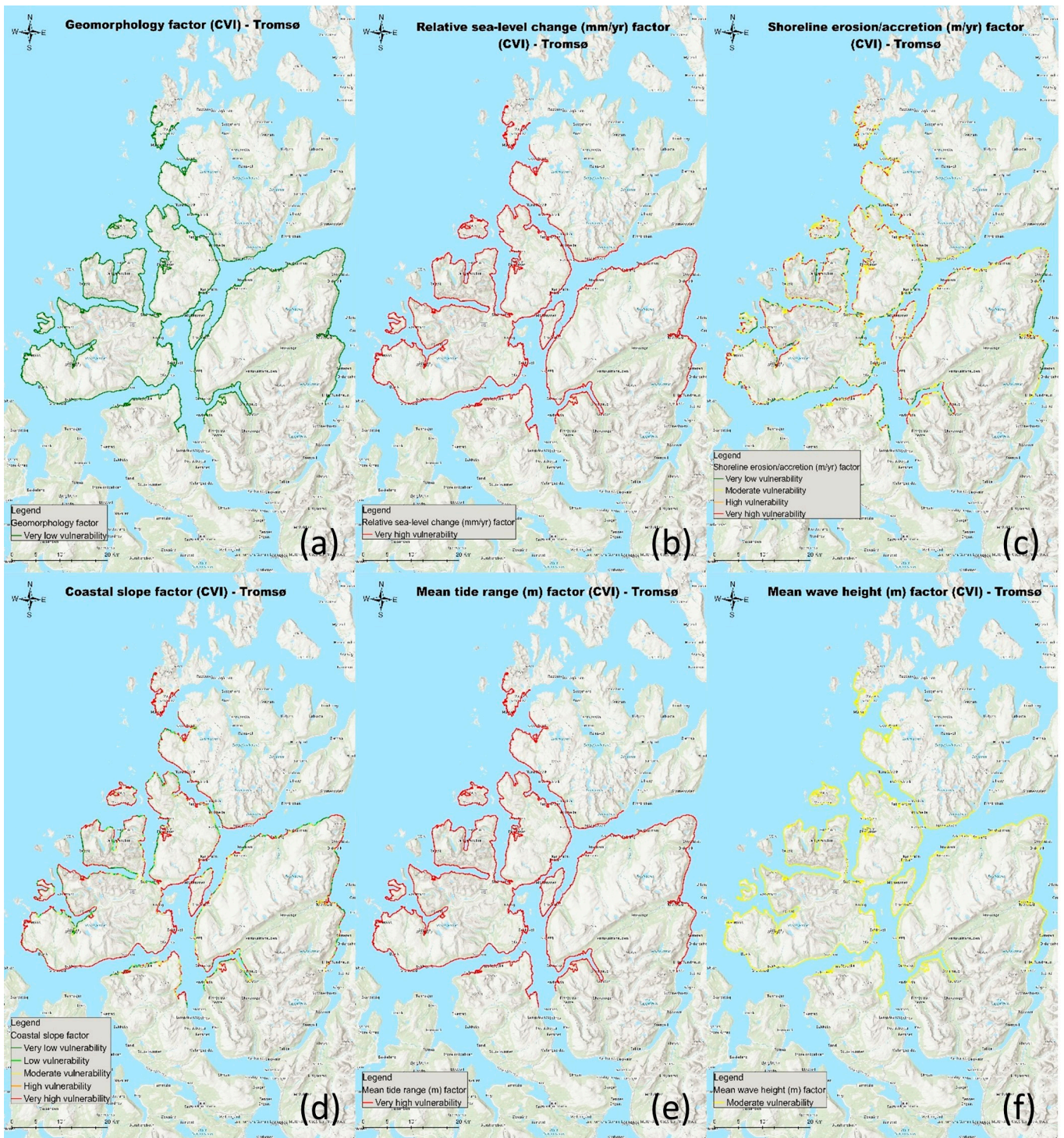

|	Geomorphology	Coastal Slope (°)	Relative sea-level change (mm/yr)	Shoreline erosion/accretion (m/yr)	Mean tide range (m)	Mean wave height (m)
Very high	0	49.1	100	20.26	100	0
High	0	3.56	0	1.86	0	0
Moderate	0	9.27	0	55.35	0	100
Low	0	10.69	0	0	0	0
Very low	100	27.38	0	22.53	0	0

Figure 3. Vulnerability of each parameter of CVI (%).

Figure 4. Vulnerability of each parameter of CVI (**a**) geomorphology, (**b**) relative sea level change, (**c**) shoreline erosion/accretion, (**d**) coastal slope, (**e**) mean tide range, and (**f**) mean wave height. The different levels of vulnerability are shown using a bivariate color palette, with red color hues indicating a high degree of vulnerability while green hues show a low level of vulnerability.

Regarding the coastal slope factor, as can be seen from Figure 4d, the vulnerability along almost the entire length of the coastline is very high. There are few points where the vulnerability is very low or low. On some parts of the coastline, mainly on the part of the coastline located to the east of the island of Tromsø, the vulnerability is moderate. Specifically for the island of Tromsø, the vulnerability along almost the entire length of the

coastline is very high with reference to the coastal slope factor. Lastly, concerning the factors of (a) geomorphology, (b) relative sea level change, (e) mean tide range, and (f) mean wave height (Figure 4a, Figure 4b, Figure 4c, Figure 4e, and Figure 4f respectively), the value is the same for the entire length of the coastline. Specifically, for the factor of geomorphology, vulnerability is very low; for the factor of relative sea level change, vulnerability is very high; for the factor of mean tide range, vulnerability is also very high; and finally, for the factor of mean wave height, vulnerability is moderate.

As can be seen from the following map (Figure 5) in combination with the corresponding diagram in Figure 6, the largest percentage of the coastline has high vulnerability, at a rate close to 37% (about 1/3 of the total coastline), while with a very small difference (at a rate of 36.65% of the total coastline), the vulnerability of the coastline is low. The moderate level of vulnerability corresponds barely to 10% of the total coastline. Finally, very high vulnerability level is found on 9% of the total coastline, while very low vulnerability on nearly 7.5% of the total coastline. Vulnerability seems to be higher in the northern part, in contrast to the southern and central parts, where lower levels of vulnerability are found. Moreover, the coastal vulnerability in the eastern part of the coast (Figure 5) is primarily low.
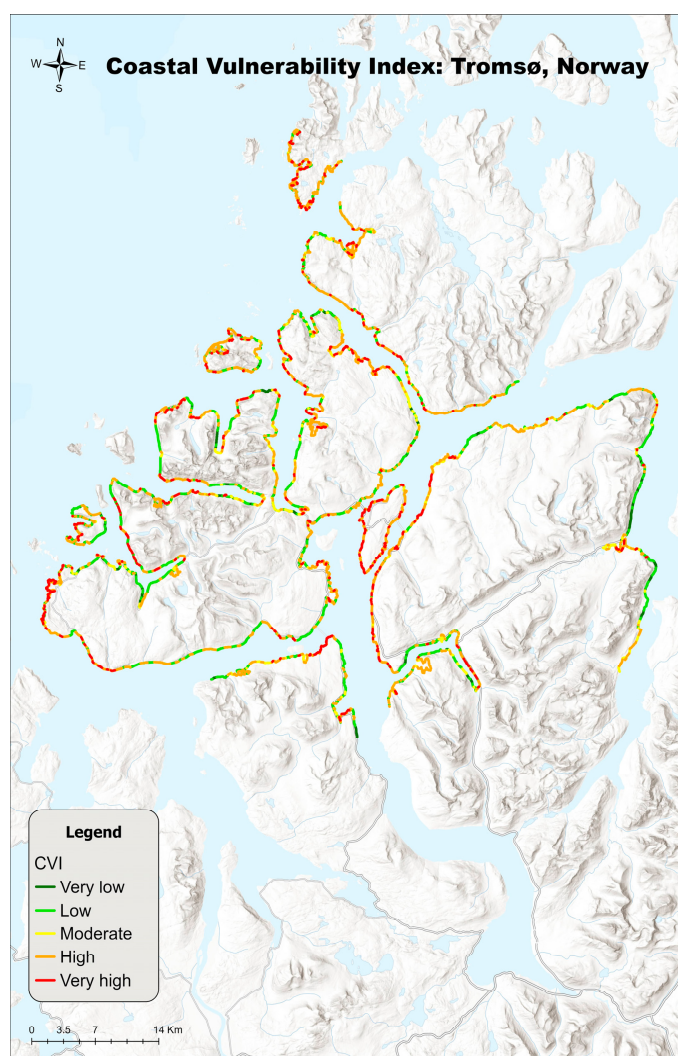
Figure 5. Map of the resulting CVI classes in the municipality of Tromsø. The different levels of vulnerability are area shown using a bivariate color palette, with red color hues indicating a high degree of vulnerability with green hues showing a low level of vulnerability.
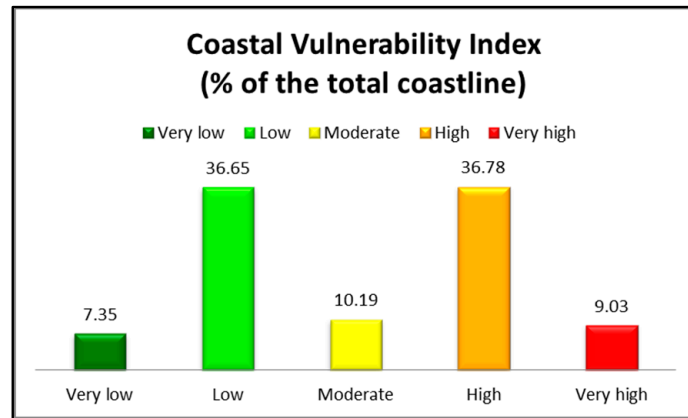
Figure 6. CVI bar chart for coastline vulnerability classes (%).

Specifically, for Tromsø Island, vulnerability is mainly high and very high. As can be seen from the map below (Figure 7), vulnerability is high mainly in the southern part of Tromsø, while in its western part, the vulnerability on some parts of the coastline is very high. Conversely, on the main northern part of the island, there are some points where vulnerability is low. In detail, the island of Tromsø demonstrates mainly high (53% of the total coastline) and very high (28% of the total coastline) levels of coastal vulnerability.
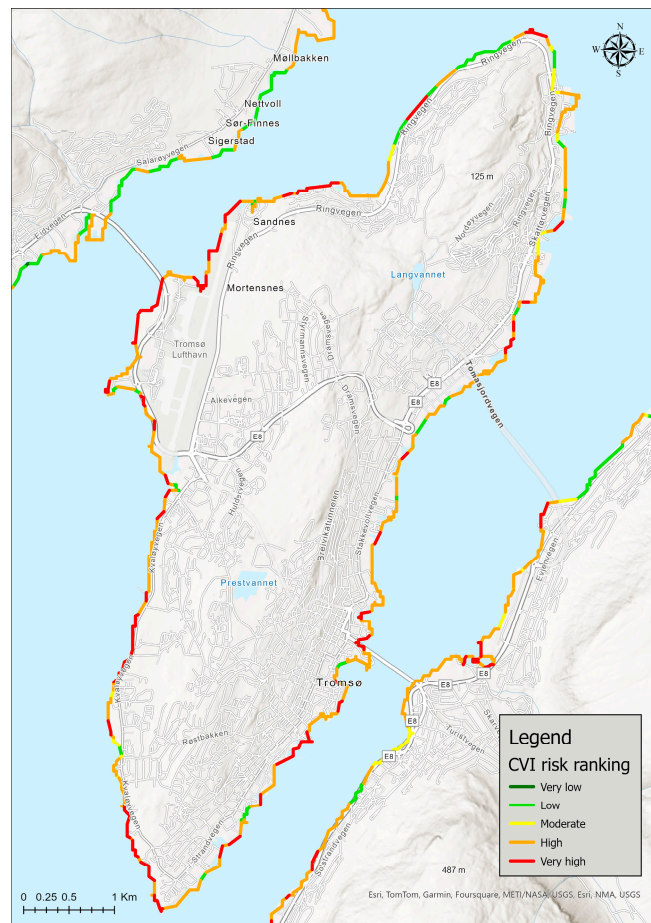

Figure 7. Coastal Vulnerability Index of Tromsø island. The different levels of vulnerability are areas shown using a bivariate color palette, with red color hues indicating a high degree of vulnerability while green hues show a low level of vulnerability.

5. Discussion

This study objective was the calculation of the CVI of the arctic coasts of the municipality of Tromsø. After the completion of the work and the application of the CVI, it appears that in the northern part of the municipality of Tromsø, the coastal vulnerability is mainly low, while in other parts of the coastline, it is high. As for the island of Tromsø, the coastal vulnerability is mainly very high and high. Erosion rates are increasing, which is the result of both anthropo-geographical and natural factors, with these two making it necessary to study them in parallel, since they are connected to each other [9].

As can be seen from Figure 3, the most important factors affecting CVI are relative sea level change and mean tide range as the vulnerability is very high along the entire length of the coastline. Then, equally important factors are the coastal slope and shoreline erosion/accretion, as in the greater part of the coastline the vulnerability is very high. Finally, to a significant extent, the factor of the average wave height significantly affects the index, since the vulnerability, as can be seen from Figure 4f, is moderate. The factor that is less important compared to the other factors is geomorphology, since the vulnerability on the whole of the coastline is very low. Similar research that was carried out in Finland [10] shows that the geology of the coasts is also of low vulnerability. Regarding wave height, as the perennial sea ice continues to melt and at the same time the duration of open water extends, ocean waves are becoming more prevalent in the Arctic Ocean [4,35], thus justifying the importance of this specific factor.

Optical data are mainly used for this type of research. However, optical data face noteworthy boundaries due to the augmented cloud cover in the circumpolar Arctic as well as the coarse spatial resolution. Likewise, since 2014, Synthetic Aperture Radar (SAR) imagery data have been available principally from the Sentinel-1 satellite [9]. During the process of calculating the coastal vulnerability, there were some issues that needed to be addressed. Specifically, a significant challenge was identified in finding suitable optical satellite imagery for estimating coastal erosion/accretion rates, due to high cloud cover, as was expected because of the nature of this data, as has already been mentioned. This challenge could be addressed by using SAR data which are available [9].

Another limitation arises from the methodology used to map coastlines and erosion in Arctic regions. More specifically, the factors (geomorphology, coastal slope, mean tide range (m), shoreline erosion/accretion (m/yr), relative sea level change (mm/yr), and mean wave height (m)) used to calculate coastal vulnerability had the same degree of gravity, which might not be the case in the real world. It is therefore necessary to give a different weight to each of those factors used to calculate coastal vulnerability, so that the results are more accurate [9]. One of the strengths of this work is the use of the CVI, the results of which can be used to identify the most vulnerable parts of the under-study coastline and to take measures to address or avoid possible problems, such as the retreat of coastline. In addition, through this specific research, the study can be taken a step further, and socio-economic indicators could be included to study the anthropo-geographic part, in addition to the physical geography.

Our results showing the high vulnerability of the Tromsø Island coastal region are in line with other studies [36]. In other Arctic regions, it appears that coastal vulnerability is mostly moderate. In more detail, in Longyearbyen on Svalbard, it appears that the most vulnerable areas are the Longyearelva Delta, while higher erosion values are found along the cliffs east of the Longyearelva Delta, which are human-altered sections. After the calculation of CVI, the results showed vulnerability that ranged from very low to high. More analytically, on the delta coast of Longyearelva, the high vulnerability is related to the low coastal slope of the delta system as well as the possible rise of erosion because of the limited sediment supply. The change of geomorphology, as well as the slope of the coastal zone, because of human actions, like the build-up of artificial coast while constructing the new port and roads, had a crucial role in the change to the shoreline and by extension the CVI [28]. The specific index has also been calculated for the Eastern Gulf of Finland coastal zone (the Baltic Sea). In this particular study, moderate vulnerability was also found on a

large part of the coastline under study, while in several parts, the coastline was low [10]. Another similar study has been conducted on the Croatian coast of Istria. With the coasts of Croatia and Istria being mostly rocky and with limestone and dolomites being their key composition, the effect of erosion is restricted. Moreover, coastal slope, elevation, and landform are critical variables because of the rising sea level in the Adriatic [37].

According to Sulikowska et al., the winter cold extremes in Alaska are decreasing at a much faster rate than summer warm extremes are increasing [38]. Moreover, the rise in wave activity has played a vital role in the increase of coastal hazards. Those hazards are frequently connected to different weather events like Arctic cyclones and strong wind events, leading to high waves and storm surges, leading to coastal flooding and accelerated erosion [39]. Glacier retreat produces large amounts of unconsolidated sediments and unstable glacial landforms. Those are exposed to the effects of waves, tides, and currents, so those areas are highly susceptible to intense erosion [40].

6. Conclusions

The aim of the present work was the calculation of coastal vulnerability on the shores of the municipality of Tromsø. Through this specific research, the study could go a step further, including socio-economic data, so that there are records not only regarding the vulnerability of the coasts but also how much the population living in these areas is affected. In conclusion, after analyzing the data, the coastline in the northern part of Norway seems to have high and low vulnerability, while specifically on the island of Tromsø, which is also the study area, the vulnerability mostly ranges from high to very high.

The results of this study show ranges from high to very high vulnerability along almost the entire coastline, so special importance should be given to those areas as well as to the population that lives there and to what extent it is likely to be affected in the present as well as in the future. The expected contribution of the study is a moderate to high vulnerability on the coast of the northern part of the Tromsø municipality because of the sea level rise and the material of the rocks of the study area, which is not so erosive. Results can be of a practical use for evaluating coastal vulnerability on the Arctic coasts and can support decision making regarding coastline management in those regions.

Regarding the future work of this study, an attempt will be made to integrate socio-economic data, in order to study how and to what extent the population living on the coastline is affected, especially in the most vulnerable areas. In addition, different weightages to the input variables for generating CVI will be given, in order to make a comparison with the results of the present research. This index is also known as the Arctic Coastal Hazard Index (ACHI). The aim of this research will be also to compare the CVI (Coastal Vulnerability Index) and ACHI (Arctic Coastal Hazard Index). The results of the specific work could actually be used in next research which will also include socio-economic data, in order to calculate how much the population living along the coastline can be affected. A possible error with the use of this index is the non-inclusion of frost, which covers a large part of the study area. Therefore, in the next step, an attempt will be made to calculate the index ACHI, which also includes the frost as a factor. In order to prove which of them is the most suitable for calculating coastal vulnerability in Arctic coastal areas, and particularly for Arctic Norway.

Author Contributions: Conceptualization, P.T., S.E.D. and G.P.P.; methodology, P.T., S.E.D. and G.P.P.; formal analysis, P.T., S.E.D. and G.P.P.; writing—original draft preparation, P.T., S.E.D., G.P.P., K.K. and N.G.T.; writing—review and editing, P.T., S.E.D., G.P.P., K.K. and N.G.T.; visualization, P.T., S.E.D., G.P.P., K.K. and N.G.T.; supervision, G.P.P. All authors have read and agreed to the published version of the manuscript.

Data Availability Statement: No new data were created or analyzed in this study. Data sharing is not applicable to this article.

Conflicts of Interest: The authors declare no conflicts of interest.

References

1. Nielsen, D.M.; Pieper, P.; Barkhordarian, A.; Overduin, P.; Ilyina, T.; Brovkin, V.; Baehr, J.; Dobrynin, M. Increase in Arctic Coastal Erosion and Its Sensitivity to Warming in the Twenty-First Century. *Nat. Clim. Chang.* **2022**, *12*, 263–270. [CrossRef]
2. Petropoulos, G.P.; Karathanassi, V.; Karamvasis, K.; Detsikas, S.E.; Dermosinoglou, A. Understanding and Monitoring the Dynamics of Arctic Permafrost Regions under Climate Change Using EO & Cloud Computing: The Contribution of EO-PERSIST Project. In *Geographical Information Science*; Elsevier: Amsterdam, The Netherlands, 2024.
3. Maslakov, A.; Kraev, G. Erodibility of Permafrost Exposures in the Coasts of Eastern Chukotka. *Polar Sci.* **2016**, *10*, 374–381. [CrossRef]
4. Casas-Prat, M.; Wang, X.L. Projections of Extreme Ocean Waves in the Arctic and Potential Implications for Coastal Inundation and Erosion. *JGR Ocean.* **2020**, *125*, e2019JC015745. [CrossRef]
5. Tsatsaris, A.; Kalogeropoulos, K.; Stathopoulos, N.; Louka, P.; Tsanakas, K.; Tsesmelis, D.E.; Krassanakis, V.; Petropoulos, G.P.; Pappas, V.; Chalkias, C. Geoinformation Technologies in Support of Environmental Hazards Monitoring under Climate Change: An Extensive Review. *Int. J. Geo-Inf.* **2021**, *10*, 94. [CrossRef]
6. Kim, J.-I.; Hyun, C.-U.; Han, H.; Kim, H.-C. Digital Surface Model Generation for Drifting Arctic Sea Ice with Low-Textured Surfaces Based on Drone Images. *ISPRS J. Photogramm. Remote Sens.* **2021**, *172*, 147–159. [CrossRef]
7. Soha, T.; Sugár, V.; Hartmann, B. City-Scale Analysis of PV Potential and Visibility in Heritage Environment Using GIS and LiDAR. *Energy Build.* **2024**, *311*, 114124. [CrossRef]
8. NOAA. What Is Lidar? 2024. Available online: https://oceanservice.noaa.gov/facts/lidar.html (accessed on 10 October 2024).
9. Petropoulos, G.P.; Petsini, T.; Detsikas, S.E. Geoinformation Technology in Support of Arctic Coastal Properties Characterization: State of the Art, Challenges, and Future Outlook. *Land* **2024**, *13*, 776. [CrossRef]
10. Kovaleva, O.; Sergeev, A.; Ryabchuk, D. Coastal Vulnerability Index as a Tool for Current State Assessment and Anthropogenic Activity Planning for the Eastern Gulf of Finland Coastal Zone (the Baltic Sea). *Appl. Geogr.* **2022**, *143*, 102710. [CrossRef]
11. Furlan, E.; Pozza, P.D.; Michetti, M.; Torresan, S.; Critto, A.; Marcomini, A. Development of a Multi-Dimensional Coastal Vulnerability Index: Assessing Vulnerability to Inundation Scenarios in the Italian Coast. *Sci. Total Environ.* **2021**, *772*, 144650. [CrossRef]
12. Koroglu, A.; Ranasinghe, R.; Jiménez, J.A.; Dastgheib, A. Comparison of Coastal Vulnerability Index Applications for Barcelona Province. *Ocean. Coast. Manag.* **2019**, *178*, 104799. [CrossRef]
13. Pantusa, D.; D'Alessandro, F.; Riefolo, L.; Principato, F.; Tomasicchio, G.R. Application of a Coastal Vulnerability Index. *A Case Study along the Apulian Coastline, Italy. Water* **2018**, *10*, 1218. [CrossRef]
14. Dey, J.; Mazumder, S. Development of an Integrated Coastal Vulnerability Index and Its Application to the Low-Lying Mandarmani–Dadanpatrabar Coastal Sector, India. *Nat. Hazards* **2023**, *116*, 3243–3273. [CrossRef]
15. Jaskólski, M.W.; Pawłowski, L.; Strzelecki, M.C. Assesment of Geohazardsand Coastal Change in Abandoned Arctic Town, Pyramiden. In *Cryosphere Reactions against the Background of Environmental Changes in Contrasting High-Arctic Conditions in Svalbard*; Polar Reports; Institute of Geoecology and Geoinformation, Mickiewicz University in Poznań: Poznań, Poland, 2017; Volume 2, pp. 51–64.
16. Sivertsen, B.; Friborg, O.; Pallesen, S.; Vedaa, Ø.; Hopstock, L.A. Sleep in the Land of the Midnight Sun and Polar Night: The Tromsø Study. *Chronobiol. Int.* **2021**, *38*, 334–342. [CrossRef] [PubMed]
17. Cartaxo, D.M.; Castilla, J.; Dymet, M.; Hossain, K.T. Digitalization and Smartening Sustainable City Development: An Investigation from the High North European Cities. 2021. Available online: https://ideas.repec.org/ (accessed on 10 October 2024).
18. Dermosinoglou, A.; Detsikas, S.E.; Petropoulos, G.; Fratsea, L.M.; Papadopoulos, A. Multitemporal Monitoring of Impervious Surface Areas (ISA) Changes in an Arctic Setting, Using ML, Remote Sensing Data and GEE. Zenodo. 2023. Available online: https://zenodo.org/records/10435903 (accessed on 10 October 2024).
19. Jacobsen, B.K.; Eggen, A.E.; Mathiesen, E.B.; Wilsgaard, T.; Njolstad, I. Cohort Profile: The Tromso Study. *Int. J. Epidemiol.* **2012**, *41*, 961–967. [CrossRef]
20. Ketzler, G.; Römer, W.; Beylich, A.A. The Climate of Norway. In *Landscapes and Landforms of Norway*; Beylich, A.A., Ed.; World Geomorphological Landscapes; Springer International Publishing: Cham, Switzerland, 2021; pp. 7–29. ISBN 978-3-030-52562-0.
21. Kairanov, B.; Escalona, A.; Norton, I.; Abrahamson, P. Early Cretaceous Evolution of the Tromsø Basin, SW Barents Sea, Norway. *Mar. Pet. Geol.* **2021**, *123*, 104714. [CrossRef]
22. Bishop-Taylor, R.; Nanson, R.; Sagar, S.; Lymburner, L. Mapping Australia's Dynamic Coastline at Mean Sea Level Using Three Decades of Landsat Imagery. *Remote Sens. Environ.* **2021**, *267*, 112734. [CrossRef]
23. Cao, W.; Zhou, Y.; Li, R.; Li, X. Mapping Changes in Coastlines and Tidal Flats in Developing Islands Using the Full Time Series of Landsat Images. *Remote Sens. Environ.* **2020**, *239*, 111665. [CrossRef]
24. Ghanavati, E.; Shah-Hosseini, M.; Marriner, N. Analysis of the Makran Coastline of Iran's Vulnerability to Global Sea-Level Rise. *J. Mar. Sci. Eng.* **2021**, *9*, 891. [CrossRef]
25. Boumboulis, V.; Apostolopoulos, D.; Depountis, N.; Nikolakopoulos, K. The Importance of Geotechnical Evaluation and Shoreline Evolution in Coastal Vulnerability Index Calculations. *J. Mar. Sci. Eng.* **2021**, *9*, 423. [CrossRef]
26. Universitat Hamburg Global Lithological Map (GLiM) 2024. Available online: https://www.geo.uni-hamburg.de/en/geologie/forschung/aquatische-geochemie/glim.html (accessed on 10 October 2024).

27. Nageswara Rao, K.; Subraelu, P.; Venkateswara Rao, T.; Hema Malini, B.; Ratheesh, R.; Bhattacharya, S.; Rajawat, A.S. Ajai Sea-Level Rise and Coastal Vulnerability: An Assessment of Andhra Pradesh Coast, India through Remote Sensing and GIS. *J. Coast. Conserv.* **2008**, *12*, 195–207. [CrossRef]

28. Jaskólski, M.W.; Pawłowski, Ł.; Strzelecki, M.C. High Arctic Coasts at Risk—The Case Study of Coastal Zone Development and Degradation Associated with Climate Changes and Multidirectional Human Impacts in Longyearbyen (Adventfjorden, Svalbard). *Land Degrad. Dev.* **2018**, *29*, 2514–2524. [CrossRef]

29. Fragou, S.; Kalogeropoulos, K.; Stathopoulos, N.; Louka, P.; Srivastava, P.K.; Karpouzas, S.; Kalivas, D.P.; Petropoulos, G.P. Quantifying Land Cover Changes in a Mediterranean Environment Using Lands at TM and Support Vector Machines. *Forests* **2020**, *11*, 750. [CrossRef]

30. Wilson, M.D. Support Vector Machines. In *Encyclopedia of Ecology*; Elsevier: Amsterdam, The Netherlands, 2008; pp. 3431–3437 . ISBN 978-0-08-045405-4.

31. Gaki-Papanastassiou, K.; Karymbalis, E.; Poulos, S.; Seni, A.; Zouva, C.H. Coastal Vulnerability Assessment to Sea-Level Rise Bαsed on Geomorphological and Oceanographical Parameters: The Case of Argolikos Gulf, Peloponnese, Greece. *Hell. J. Geosci.* **2010**, *45*, 109–121.

32. Cheewinsiriwat, P.; Langkulsen, U.; Lertwattanamongkol, V.; Poompongthai, W.; Lambonmung, A.; Chamchan, C.; Boonmanunt, S.; Nakhapakorn, K.; Moses, C. Assessing Coastal Vulnerability to Climate Change: A Case Study of Nakhon Si Thammarat and Krabi. *Soc. Sci.* **2024**, *13*, 142. [CrossRef]

33. Yahia Meddah, R.; Ghodbani, T.; Senouci, R.; Rabehi, W.; Duarte, L.; Teodoro, A.C. Estimation of the Coastal Vulnerability Index Using Multi-Criteria Decision Making: The Coastal Social–Ecological System of Rachgoun, Western Algeria. *Sustainability* **2023**, *15*, 12838. [CrossRef]

34. Theocharidis, C.; Doukanari, M.; Kalogirou, E.; Christofi, D.; Mettas, C.; Kontoes, C.; Hadjimitsis, D.; Argyriou, A.V.; Eliades, M. Coastal Vulnerability Index (CVI) Assessment: Evaluating Risks Associated with Human-Made Activities along the Limassol Coastline, Cyprus. *Remote Sens.* **2024**, *16*, 3688. [CrossRef]

35. Frederick, J.M.; Thomas, M.A.; Bull, D.L.; Jones, C.A.; Roberts, J.D. *The Arctic Coastal Erosion Problem*; Sandia National Laboratories: Albuquerque, NM, USA, 2016.

36. Breili, K.; Simpson, M.J.R.; Klokkervold, E.; Roaldsdotter Ravndal, O. High Accuracy Coastal Flood Mapping for Norway Using LiDAR Data. *Nat. Hazards Earth Syst. Sci.* **2020**, *20*, 673–694. [CrossRef]

37. Šimac, Z.; Lončar, N.; Faivre, S. Overview of Coastal Vulnerability Indices with Reference to Physical Characteristics of the Croatian Coast of Istria. *Hydrology* **2023**, *10*, 14. [CrossRef]

38. Sulikowska, A.; Walawender, J.P.; Walawender, E. Temperature Extremes in Alaska: Temporal Variability and Circulation Background. *Theor. Appl. Clim.* **2019**, *136*, 955–970. [CrossRef]

39. Henke, M.; Miesse, T.; de Lima, A.D.S.; Ferreira, C.M.; Ravens, T.M. Increasing Coastal Exposure to Extreme Wave Events in the Alaskan Arctic as the Open Water Season Expands. *Commun. Earth Environ.* **2024**, *5*, 165. [CrossRef]

40. Kavan, J.; Strzelecki, M.C. Glacier Decay Boosts the Formation of New Arctic Coastal Environments—Perspectives from Svalbard. *Land Degrad. Dev.* **2023**, *34*, 3467–3474. [CrossRef]